LAWRENCE
LIVERMORE
NATIONAL
LABORATORY

UCRL-TR-213721

Measurement and Modeling of Resistivity as a Microscale Tool to Quantify the Volume Fraction of Lenticular (alpha)' Particles in a Partially Transformed (delta)-phase Pu-Ga Matrix

J. J. Haslam, M. A. Wall, D. L. Johnson, D. J. Mayhall, A. J. Schwartz

July 19, 2005

This work was performed under the auspices of the U.S. Department of Energy by University of California, Lawrence Livermore National Laboratory under Contract W-7405-Eng-48.

Measurement and Modeling of Resistivity as a Microscale Tool to Quantify the Volume Fraction of Lenticular α′ Particles in a Partially Transformed δ-Phase Pu-Ga Matrix

Jeffery J. Haslam, Mark A. Wall, David L. Johnson, David J. Mayhall, and Adam J. Schwartz
Lawrence Livermore National Laboratory, 7000 East Avenue, Livermore, CA 94550

ABSTRACT

We have measured and modeled the change in electrical resistivity due to partial transformation to the martensitic α′-phase in a δ-phase Pu-Ga matrix. The primary objective is to relate the change in resistance, measured with a 4-probe technique during the transformation, to the volume fraction of the α′ phase created in the microstructure. Analysis by finite element methods suggests that considerable differences in the resistivity may be anticipated depending on the orientational and morphological configurations of the α′ particles. Finite element analysis of the computed resistance of an assembly of lenticular shaped particles indicates that series resistor or parallel resistor approximations are inaccurate and can lead to an underestimation of the predicted amount of α′ in the sample by 15% or more. Comparison of the resistivity of a simulated network of partially transformed grains or portions of grains suggests that a correction to the measured resistivity allows quantification of the amount of α′ phase in the microstructure with minimal consideration of how the α′ morphology may evolve. It is found that the average of the series and parallel resistor approximations provide the most accurate relationship between the measured resistivity and the amount of α′ phase. The methods described here are applicable to any evolving two-phase microstructure in which the resistance difference between the two phases is measurable.

Keywords: plutonium, electrical resistivity/conductivity, polyphase microstructure, polymorphic phase transformations, finite element analysis

INTRODUCTION

The element plutonium has the distinction of exhibiting 6 allotropic phases between room temperature and the liquid state [1]. In unalloyed plutonium, the face centered cubic δ phase is stable between 325°C and 460°C. However, the δ phase can be retained in a metastable state at room temperature by additions of various alloying elements such as Al, Ce, Ga, In, Zn, and others [1]. On cooling, the retained δ phase undergoes an isothermal martensitic phase transformation to produce lenticular α′ particles [2 - 6]. Here, the α′ designation indicates the monoclinic crystal structure, similar to unalloyed α, but with the presence of Ga resulting in a change in lattice parameters. The α and α′ phases are approximately 20% higher in density in comparison to the δ phase. This large volume (density) change during the transformation likely leads to considerable elastic and plastic deformation to accommodate formation of the α′ particles and is thought to make a significant contribution to the rather large, ~130°C hysteresis in the transformation [7].

Dilatometry has been used to characterize the δ to α′ phase transformation in plutonium [2, 3, 5, 8]. The hazards and difficulties associated with working with Pu metal make it prudent, and sometimes necessary, to work with very small quantities of the material. However, standard push-rod dilatometers do not have sufficient accuracy to measure the change in thickness due to a partial transformation in very thin specimens. Although other dilatometry techniques may be possible, we have chosen electrical resistivity to characterize the martensitic transformation. Resistivity has been used previously to measure defect accumulation and annihilation during isochronal (equal time at successive temperatures) annealing experiments [9], phase transformations in unalloyed plutonium [2, 10], and more particularly has been used to follow the δ to α′ phase transformation in alloys of δ-phase Pu retained at room temperature by the addition of Al or Ga [11 - 13]. The samples used in this investigation are disks, 2.8-mm in diameter and approximately 125 to 150 μm thick (a standard transmission electron microscopy (TEM) foil size before thinning for electron transparency). The advantage of this geometry is that the same sample can be characterized with TEM after completion of the electrical resistivity experiment. The negative attribute of this geometry is that it does not allow for a standard resistivity measurement arrangement and thus requires additional simulations to accurately interpret the data. In particular, the cross-section width is non-uniform when resistivity is measured across the width of the disk sample. To validate the 4-probe resistometry technique for these specimens, we have performed a finite element analysis of resistivity with a disk sample geometry.

The δ to α' phase transformation in plutonium is readily detectable with resistivity because the α phase has a resistivity that is approximately 45% greater than the δ phase at room temperature and continues to remain significantly greater than that of the δ phase over the temperature range where the forward and reverse transformations occur [1]. The usual interpretation of the resistance data during the transformation is to apply a linear approximation to the amount of α' formed based on the difference between the resistivity of the pure α and alloyed δ materials (in the case of δ, extrapolated to low temperatures) [3, 11]. The linear approximation basically represents the microstructure during the transformation in terms of a connection of the α' and δ phase regions as resistors in series, as illustrated in Figure 1(a). We believe that the series resistor approximation likely underestimates the amount of transformation in the sample because the isolated α' particles are dispersed as lens or lenticular shapes within the interconnected δ phase. It is well known that the resistivity of the same resistors in a parallel circuit will be lower than the series circuit. As also illustrated in Figure 1(a), an arrangement of continuous α' phase oriented parallel to the current will result in a lower bound of the resistivity. To evaluate which, if either of these two bounds applies to the partially transformed Pu-Ga alloy, a two-dimensional analysis of the resistivity is also performed using a finite element technique for a simulated microstructure containing the lenticular-shaped α' phase. This analysis should be reasonably valid for evaluating two-phase microstructure evolution in any system with differences in resistivity and reasonably similar microstructures. In particular, results are presented to compare simulations of microstructures with a known amount of α' to the amount of α' phase that would be assumed to be present based on the series resistor approximation.

EXPERIMENTAL

Nominally Pu-0.6 wt. % Ga alloys have been prepared by casting, cross rolling, and heat treating to improve homogeneity. Standard metallographic techniques are used to prepare samples for optical microscopy, x-ray diffraction, and resistivity measurements. The challenges of using 2.8-mm diameter disks for resistivity measurements are offset by the ability to characterize small samples of Pu alloys more easily. Resistivity measurements are made with a 4-probe (also called Kelvin probe) resistance measurement technique. Wires are used as contacts on one face of the disk sample and arranged on top of the sample as shown in Figure 2. The wires are placed parallel to each other on the surface and the spacing distances perpendicular to the wires were 0.330, 1.930, and 0.330 mm, respectively. The outer wires are used for the current probes and the inner wires are used to sense the voltage drop across the sample.

Resistivity samples are attached to a helium cryostat to perform resistivity measurements during cooling and heating. The samples are prepared by electro-polishing in a controlled atmosphere glove box and are pressed against the wires described above by a spring loaded mechanism to maintain contact during the experiments. Cooling is controlled with cartridge heaters attached to the cryostat. The cryostat is located in a vacuum chamber, which attained less than 10^{-6} torr during experiments. The temperature is monitored with 100 Ohm platinum Resistance Temperature Detector (RTD) sensors (Lake Shore Cryotronics, Inc., Model PT-103, Westerville, OH) attached directly beneath the samples. The disk samples are mounted in a glass-ceramic fixture. The RTD sensors allow measurement over the temperature range of experiments, 25K to 700K.

X-ray Diffraction (XRD) measurements are made with an INEL CPS120 (Artenay, France) which has a multi-channel detector with a range of 120 degrees. A sample holder with polyimide windows over the sample is used to prevent the spread of contamination. To model the resistivity of this disk shaped sample configuration, a finite element analysis package (Maxwell 3D Field Simulator, Version 5, Magnetostatic DC Conduction Module, Ansoft Corporation) is used to calculate the effective width of the circular sample and thereby obtain an absolute resistivity value.

RESULTS AND DISCUSSION

Optical Microscopy

An optical micrograph of a Pu-Ga specimen quenched and held at –118°C for 1000 seconds is shown in Figure 3(a). The α' particles appear as elongated dark particles on a lighter background using the differential interference contrast technique [14]. The volume fraction of α' particles in the micrograph in Figure 3(a) is 6.9 volume % with an aspect ratio of approximately 9. The average thickness of the lenticular-shaped α' particles is 0.9 µm. The arrangement of α' particles shown here is also typical of a sample that was cooled to –120°C and heated to room temperature at a constant rate of 20°C/min as shown in Figure 3(b). These results confirm similar observations made by Zocco et al. [15] of the lens shaped features of the α' phase within the δ microstructure of the plutonium alloy. The δ phase grains are observed to contain certain preferred orientations or variants of the α'. Careful analysis of optical images using an assumed crystallographic relationship between the α' and δ phases suggests that 4 variants may be observed in a planar section (however, often all 4 are not easily distinguishable) [16]. It sometimes appears that one or more of these variants can dominate in terms of volume fraction over the others. Thus, an orientation dependence of the resistivity of the grain microstructure may be relevant for the determination of the amount of phase present.

X-Ray Diffraction Measurements

In a comparison study using a technique developed by Jackson and Pinkney [17], an X-Ray Diffraction (XRD) measurement has been used to determine the amount of transformation. The amount of α' phase observed with this XRD technique was similar to the amount determined by resistivity measurements using the correction described later. The XRD measurement gave 20.0 atomic % α'. This approach determines the amount of α' from ratios of the integrated peak intensities for the α' and the δ phase and is believed to be insensitive to alloy composition and the temperature at which the α' is formed. XRD on the starting material indicated an all delta-phase sample, i.e., no surface α'.

Finite Element Analysis of Resistivity of a Disk

Finite element analysis (FEA) is first utilized to validate the electrical resistivity measurement with the 4-probe technique on small disk shaped specimens. The analysis indicates that the current spreads rather uniformly between the inner (voltage) probes and through the sample thickness with some perturbations at the locations of the current and voltage probes. An example of an FEA simulation of the current flow through the disk is shown in Figure 2. The effective width that is calculated is 1.8853 mm for typical properties of the sample and varies 0.5% or less for expected variations in the resistance of the sample. At most, a 2% error is possible with misalignment of the electrical probes on the sample, but this would be a relative error only since it is expected the probes should not move during the experiments. From these simulations, we conclude that this measurement technique is adequately sensitive to the resistivity changes so that the amount of the α' phase formed during the transformation can be determined.

Resistivity Measurements

Resistivity measurements obtained during the transformation using 4-probe resistivity measurement on the disk sample are plotted in Figure 4. These results are qualitatively similar to previous work by Elliott et al. [12] and Joel et al. [13]. An example of multiple cycles through the phase transformation temperatures is shown in Figure 4(b). It can be seen that the resistivity is reproducible at a given heating and cooling rate. Although radiation damage effects can affect resistivity measurements particularly on the first cooling and heating cycle for an aged sample, the effect is minimal when temperature cycles are repeated without significant interruption.

Finite Element Analysis of Effects of Particle Orientation

To quantify the relationship between resistivity changes measured during the δ to α' phase transformation and the volume fraction of α', a finite element analysis of the change in resistivity using some postulated model grains with lens shaped particles of α' is performed. Lens shaped particles are selected to approximate the observed α' particles such as those seen in Figure 3(a) and (b). Alternatively, these square shaped "grains" can be treated as portions of a grain that are combined together to make a grain, but from here on they will be referred to as grains. This approach is an approximation limited to a two-dimensional analysis of lens shaped α' phase particles within a square grain of δ. The modeling of resistivity of the grains uses the same software mentioned above. Some examples of these configurations are shown in Figure 5. An array of randomly transformed grains is analyzed as a resistor network with conduction through all four sides.

The resistance of a network of 100 square grains (10 x 10 array) is determined by analyzing the network of resistors with resistance in each direction determined by the resistivity calculated from the finite element simulation of each grain. An illustration of this is shown in Figure 1(b). The orientations of the grains within the network are assigned randomly at 0° and 90° unless otherwise constrained by the analysis. Various simulations are attempted; the amount of α' in the grains as well as the number of δ grains containing α' are also assigned randomly depending on the desired simulation. The resistance is calculated between the top and the bottom of the 10 by 10 array of grains with the top and bottom edges each having an equipotential surface along their lengths. The two sides of the array are connected (periodic boundary condition). A Gauss-Seidel iteration [18] is used to obtain the resistance of the network.

Iterations are continued nominally to the precision limit of the software and the resulting standard deviation in the current at any cross-sections between the top and bottom is less than 1 ppm. The resistance calculated from the simulation is used to calculate a volume fraction of α' that would be expected if the series approximation for resistivity is assumed. The actual volume fraction of α' in the simulation is recorded for comparison. Additional versions of the configurations of lens shaped particles are shown in Figure 6. In some of these simulations, the lens shapes are increased in size to approximate the growth of the particles. Although the α' phase likely grows from a grain boundary, precipitates, or other defects, this simulation includes the α' growing from the centroid of lens shape. This approach is taken to develop a model to approximate the resistivity of an evolving two-phase microstructure composed of lenticular precipitates. Typically, 100 randomly assigned "microstructures" are generated for each simulation condition to produce data for a range of total α' phase in the microstructure.

The difference between the amount of α' phase in the simulation and the amount of α' that would be assumed to be present from the series resistor approximation is plotted against the amount of α' in the simulation in Figures 7 (a) – (c). In Figure 7 (a), a comparison of the series approximation for the model δ grain shown in Figure 5 (a) indicates that the underestimation in the amount of α′ is significant when the grains are allowed to have random orientations. The two additional sets of data in Figure 7 (a) show the difference from the series resistor approximation when all the grains containing the α′ are forced to have one or the other orientation. When the orientations are forced to be the same, the scatter in the results is significantly smaller. The random orientation of the transformation within the grains clearly contributes significantly to the scatter. The scatter is also produced by both the statistical probability associated with the clustering of partially transformed grains near each other and the blocking of current flow by rows of adjacent grains containing α′. In this particular simulation, there is considerable difference in the resistivity in the vertical and horizontal directions.

When random probability allows for more grains of one orientation to form in the array, variations from the average are observed. It is expected that with a larger network of grains (greater than 10 x 10 network) this scatter should converge. It is also observed that when very few grains contain α′ particles (i.e., as volume fraction approaches zero) that the majority of the grains could have similar orientations. In these cases, the few grains that transform may cause anomalously large or small differences between the volume fraction of α′ in the simulation and amount of α′ determined using the series approximation. This can explain the large scatter in the data approaching zero volume fraction of α′ phase.

Figure 7(b) shows additional results for analyses of grains that have one-third and two-thirds of the amount of α′ (by volume) as that in the grains from Figure 7(a). These are approximations to a transformation process with the α′ particles growing within the δ grain. For these grains, the α′ particles were taken to expand from their centroids. These centroids remained fixed in all the simulated δ grains. The small differences in the results for the 1/3 and 2/3 lens sizes compared to the full size lens can be attributed to the actual differences measured in the resistivities of these model grains. It can be expected that the difference in actual α′ and α′ determined from series resistor approximation in resistivity should disappear as the volume fraction of α′ particles approaches zero, but this is not directly observed due to the scatter in results as mentioned earlier. In these simulations with smaller α′ particles, the resistivity for these model grains scales with the amount of α′ phase within the grain but the overall average resistance (from both the horizontal and vertical directions) is still significantly lower than that obtained from the series resistor approximation.

Figure 7 (c) shows a case where a δ grain contains eleven α′ lens shaped particles, shown in Figure 5 (b), that are fairly uniformly distributed throughout the grain. In this simulation, it turned out that the resistivities in the two directions are nearly equal. Consequently, the scatter in the plot is rather small for this simulation. In this simulation the grain with 11 lens shaped α′ phase particles in the δ grain has a resistivity that is about 14% less than what would be predicted by a series resistor approximation.

Finite Element Analysis of Effects of Evolving Microstructure

It is possible to simulate microstructures where the δ grains have any volume fraction of α′ phase between zero and the maximum α′ volume fraction for that particular simulated grain by using a fit to resistivity as a function of the volume fraction of α′. Figure 7 (a) and the first two images in Figure 6 are examples of evolving microstructures that are considered. Evolving microstructures based on some of the other microstructures in Figure 6 are also considered. The fits are generally linear with volume fraction and are constrained to pass through zero. It is possible that this is not accurate at very low volume fractions, $<<0.01$, but the linear fit overall is good. To consider the evolution of the α′ microstructure, several variations in the simulations utilizing the 10 x 10 network of grains are performed. Table 1 indicates the modifications to the simulations. In some cases, limits are applied to the maximum amount of transformation in any grain or to the minimum transformation of any grain. These simulations are performed to consider possible paths for the evolution of the microstructure with continuing transformation. In the case of a limiting maximum amount of transformation, the simulation represents an early stage of the transformation where the α′ plates are growing progressively into the δ grains in the microstructure (Simulation 2 in Table 1).

The simulations where a minimum amount of transformation per grain is specified are intended to approximate transformation conditions where the α′ plates fully develop rapidly in a given grain. This is intended to reflect the later stages of the transformation where there are few if any δ grains that do not have significant amounts of α′ phase within them. Simulation 3 in Table 1 is an approximation to this condition. In the simulation where it is randomly assigned whether a grain will transform at all (Simulation 4 in Table 1), the minimum transformation requirement reflects a spontaneous transformation of some but not all of the grains. The simulation in this example is used to approximate a transformation in the δ grain that goes to some level of transformation rapidly and stops (since the α′ transformation usually does not fully transform the grain). Some untransformed grains are present in the simulation, which might transform at later times. Similarly, Simulation 5 utilizes a fixed amount of α′ formed in each δ grain but not all the grains transform. More combinations of simulations are possible which are not described, but those in Table 1 are chosen as representative cases to explore the effects of the possible paths of the transformation process on the relationship between the resistance measured and the actual amount of α′ within the sample. Because it is not certain exactly how the transformation progresses, these simulations are attempted with the aim of obtaining bounding cases for the relationship between the observed resistivity and the amount of α′ phase that has formed.

Figure 8 shows the combined results from the simulations in Table 1. The various simulations attempted in Table 1 nominally produce a similar relationship between the resistivity and the amount of α′ in the microstructure at least within the limit of the amount of variability in the data. This gives confidence in concluding that the details of the evolution of the α′ morphology within the δ grains do not have a significant impact on inferring the amount of α′ phase from the measured resistivity. The series resistor approximation relationship is also shown in Figure 8 and the combined data clearly are different from the series resistor approximation. There is a reasonable linear fit through the combined results for up to ~0.2 volume fraction, but this linear fit is not the same as the series resistor approximation. The slope of this fitted line provides a correction over the relatively low volume fraction range (< 0.30 fraction α′). The rule of mixtures or series resistor approximation still does not accurately reflect the observed data. The parallel resistor approximation also does not fit the data. Some other models of composite behavior can be considered. One that provides a relationship between conductivity and volume fraction of dispersed conducting particles (particle composite model) includes non-linear terms [19]:

$$Composite \quad Conductivity = \quad k\frac{(1-v)}{\left(1+\frac{v}{2}\right)}; \qquad (1)$$

k is approximately equal to the conductivity of the matrix (more continuous) phase,
v is the volume fraction of the non-conducting (particulate) phase.

This relationship is shown in Figure 8 with the unspecified constant adjusted to fit the low volume fraction portion of the data. The particle composite model is clearly not appropriate which could be attributed to the assumptions of large differences in the resistivity of the two phases (i.e., one more conducting and the other negligibly less conducting) and an assumption of equiaxed particles (such as a spherical shape).

An alternate possibility is an average of the series and parallel resistor approximation. In this case, the implicit assumption is that the microstructure is divided into regions of parallel rectangular plates of α′. Although these packets of plates would be expected to be randomly oriented, an appropriate simplified approximation could be a series combination of the two microstructures as shown schematically in Figure 9. In this case, the resultant resistance is equivalent to the average of the series resistor and parallel resistor approximations. Random amounts of α′ phase were simulated with a simple flat parallel plate microstructure such as that shown in Figure 9 using the 10 x 10 network of resistors. As shown in Figure 10, the results do agree well with the average of the series and parallel resistor approximation. Figure 11 shows that the average of the series and parallel resistor approximations also provides a good fit to the pooled data from the simulations. As mentioned earlier, a simple linear fit to the results from the simulations also provides a reasonable relationship between the measured resistivity and the amount of α′ phase present in the microstructure for low volume fractions. However, the average of the series and parallel resistor approximation does have a fundamental basis that is supported by the postulated microstructure shown in Figure 9. This relationship would expected to be valid and would have greater accuracy for higher volume fractions of α′ phase. Such a relationship would be represented as follows:

$$R_{total} = V_\alpha \frac{R_\alpha}{2} + (1-V_\alpha)\frac{R_\delta}{2} + \left(\frac{1}{2\frac{V_\alpha}{R_\alpha} + 2\frac{1-V_\alpha}{R_\delta}}\right) \qquad (2)$$

where V_α = volume fraction α′, R_α = resistivity of α′ phase,
R_δ = resistivity of δ phase, and R_{total} = resistivity of the composite microstructure.

Comparison of model to X-Ray diffraction

For comparison, a single XRD measurement was available which indicated 20.0 atomic % α′ in the sample compared to 20.8 atomic % obtained by the corrected (average of series and parallel approximation) resistivity measurement for the same sample. If the series approximation were used the amount would have been 17.7 atomic %, a difference of 15%. The use of the corrected resistivity measurement yields an amount of α′ phase much closer to the amount measured by XRD. The magnitude of the correction in amount of α′ becomes bigger as the volume fraction of α′ increases; although as the amount of α′ increases the percent error (relative to the amount of α′) decreases to about 10 % at 50 atomic % α′. In the Pu-Ga system the amount of α′ is often 30 % or less [2, 3], except in alloys with ≤1.4 atomic % Ga, where it may reach 50% or more [3].

SUMMARY

We have followed the progress of the δ to α′ phase transformation in a Pu-Ga alloy by a resistivity technique, using a 2.8 mm disk sample and a 4-probe arrangement. Simulations by a finite element method of the postulated configuration of lens shaped α′ particles within model δ grains (or portions of a grain) suggests that considerable anisotropy in the resistivity may occur depending on the arrangement of the lens shaped α′ particles within the δ grains. Additionally, even in simulated microstructures with minimal anisotropy in the resistivity, it is observed that the resistivity of lens shaped particles is not predicted by a simple series resistor approximation. In this study, the resistivity of the partially transformed grains departs from the series resistor approximation and can lead to significant differences in the predicted amount of α′ phase present in the microstructure. An underestimation of the amount of α′ in the sample by as much as 15%, or more, appears to be possible. It is observed that an average of the simple series and parallel resistor approximation provided a good fit to the simulated microstructures in this work and likely would be even more important at higher volume fractions of the second phase. Further, the resistivity calculated from simulations using simple parallel plate arrangements of the α′ and δ phase as grains in the microstructure produce similar results to the simulations of lens shaped α′ microstructure. This suggests that the lenticular shapes considered in this work may be approximated well by simple rectangular plates. It is also observed that simulations to consider the effect of the various α′ transformation paths for the evolution of the lenticular α′ particles in the δ grains did not produce significant differences in the resistivity for a given amount of α′ phase. It is inferred that this resistivity technique is insensitive to transformation path taken as the α′ phase forms. Use of an x-ray diffraction technique to characterize the amount of α′ phase in a microstructure that was also measured by resistivity indicates the correction suggested by this work is appropriate. Although this analysis has been developed for the martensitic transformation in Pu-Ga, the approach is generally applicable to development of any two-phase microstructure particularly when one of the phases has a lenticular morphology.

ACKNOWLEDGEMENTS

This work was performed under the auspices of the U.S. Department of Energy by the University of California, Lawrence Livermore National Laboratory under contract No. W-7405-Eng-48.

REFERENCES

[1] Miner WN and Schonfeld FW. In Wick OJ, editor. "Physical properties," Plutonium handbook. New York NY: Gordon and Breach, Science Publishers, Inc., 1967. pp. 31-57.
[2] Faiers ME, Loasby RG, Ward BJ, Orme JT and Spicer BR. Transformation kinetics of the α–β and δ–α transitions in pure and alloyed plutonium. In Kay AE and Waldron MB, editors. Plutonium 1965 London: Chapman and Hall, 1967. pp. 64-87.
[3] Orme JT., Faiers ME, and Ward BJ. The kinetics of the delta to alpha transformation in plutonium rich pu-ga alloys. In Blank H and Lindner R, editors. Plutonium 1975 and other actinides. New York NY: American Elsevier, 1976. pp. 761-773.
[4] Hecker SH, Plutonium and its alloys. In Cooper NG, editor. Los Alamos Science, Challenges in Plutonium Science, num. 26, Los Alamos (NM): Los Alamos National Laboratory, 2000. pp. 290-335.
[5] Mitchell JN, Stan M, Schwartz DS, and Boehlert CJ. Phase stability and phase transformations in plutonium and plutonium-gallium alloys. Metall and matrls trans A 2004; **35A**: 2267-2278.
[6] Deloffre P, Truffier JL, and Falanga A. Phase transformation in Pu-Ga alloys at low temperature and under pressure: limit stability of the δ phase. J alloys and comp 1998; **271-273**: 370 – 373.
[7] Krenn CR, Sadigh B, Schwartz AJ, and Wolfer WG. Effects of local solute ordering and plasticity on the delta to alpha transformation in gallium-stabilized plutonium alloys. In Jarvinen GA editor. Plutonium futures – the science, AIP Conference Proceedings, vol. 673. Melville (NY): American Institute of Physics, 2003. pp. 87-89.
[8] Hecker SS, Harbur, DR, and Zocco TG. Phase stability and phase transformations in Pu-Ga alloys. Prog in matrl sci 2002; 49, 429-485.
[9] Fluss MJ, Wirth BD, and others. Temperature-dependent defect properties from ion-irradiation in Pu (Ga). J alloys and comp 2004; **368**: 62-74.
[10] Sandenaw TA and Gibney RB. The electrical resistivity and thermal conductivity of plutonium metal. J phys chem solids 1958; **6**, 81-88.
[11] Anderson JW and Gilmore RR. Measurement of alpha phase plutonium in plutonium – 1 w/o gallium alloy by electrical resistivity. Los alamos scientific report, LA–3332, June 30, 1966.
[12] Elliott RO, Olsen CE, and Louie J. Electrical behavior below 300°K of plutonium-rich, delta-phase solid solution alloys containing cerium, aluminum and zinc. J phys chem solids 1962; **23**, 1029-1044.
[13] Joel J, Roux C, and Rapin M. Resistivite electrique des solutions solids d'alliages Pu-Ga en phase ∂ a tres basses temperatures (4,2-300 °K). J nucl matrls 1971; **40**: 297-304.
[14] Price CE. Differential interference contrast. In Mills K et al, editors. Metals handbook, vol. 9, 9th edition. Metals Park, (OH); American Society for Metals, 1985.
[15] Zocco, TG, Stevens MF, Adler PH, Sheldon RI, and Olson GB. Acta metall mater 1990; **38**: 2275-2282.
[16] Krenn CR, Wall MA, Schwartz AJ. Transformation crystallography and plasticity of the delta to alpha prime transformation in plutonium alloys. In Solderholm L et al, editors. Actinides--basic science, applications and technology, vol. 802. Warrendale, (PA): Materials Research Society, 2004.
[17] Jackson RJ and Pinkney RJ. X-ray method for measuring percentage of alpha in delta-stabilized plutonium alloys. Metallography 1969; **1**: 387-397.
[18] James ML, Smith GM, and Wolford JC, Applied Numerical Methods for Digital Computation, 3rd edition. Harper and Row, New York, 1985, p. 198.
[19] Lee WE and Rainforth WM. Ceramic Microstructures: Property control by processing. London: Chapman & Hall, 1994, p. 70.

TABLES

Table 1. Conditions for simulations of the continuously variable volume fractions of the α′ phase within the simulated δ grain.

Simulation number	Fixed size of α′ in each partially transformed grain	Random orientation of δ grain	Random number of δ grains that transformed	Random limit to volume fraction of α′ in a partially transformed grain	Random minimum limit to amount of α′ in a partially transformed grain
1		X	X		
2		X	X	X	
3		X			X
4		X	X		X
5	X	X	X		

LIST OF FIGURES

Figure 1. (a) These illustrations show the conceptual microstructure and resistor network for the series and parallel approximation. The resistor equivalent circuit is shown superimposed on the simulated microstructure. The thin bars on the top and bottom provide two equipotential surfaces. (b) These figures show the equivalent electrical circuit determined from a finite element simulation of a lenticular α′ microstructure. The illustration on the right shows a simulation with a 10 x 10 array of simulated grains. A resistor network with resistance values R_v and R_h obtained for each grain was used for the simulations of the microstructure. Depending on the simulation, the grains would be assigned randomly as containing transformed α′ and also in some cases the amount of α′ in the grain.

Figure 2. This figure shows a finite element simulation of the current flow through the disk. The rectangular boxes show the locations and length of the wires contacting the top of the sample for the 4-probe resistivity measurements. The highest current density is under the end (current) electrodes with intermediate current density in the middle of the disk. Less current density is found in the darker edges away from the electrodes.

Figure 3. (a) Optical micrograph of partially transformed δ grains with α′ particles revealed with differential interference contrast. White and black elongated particles are α′. Sample was held at –118°C for 1000 seconds to produce the α′ particles. The volume fraction of α′ particles in the micrograph in Figure 3(a) is 6.9 volume % with an aspect ratio of approximately 9. The thickness dimension was 0.9 μm on average. (b) This figure shows a microstructure after cooling to -120°C at ~20°C/minute to transform δ to α′.

Figure 4. (a) Resistivity measured on a Pu-Ga alloy using 4-probe resistivity on a disk sample. The resistivity of α and δ phases is also shown for reference. (b) Measurement of resistance on several cycles at 1.5K/minute for the same sample.

Figure 5. This illustration shows simulated microstructures of (a) Thin lens α′, (b) 11 lens configuration of α′. Darker areas reflect a lower current density. Dark lens shapes are the α′ which has a higher resistivity compared to the delta phase. The α′ particles are the simple lens shaped objects in these illustrations.

Figure 6. Additional α′ lens shape configurations used for further analyses. The first two were simulations of the configuration in Figure 5 (a) at earlier times in the α′ particle growth. The other four are examples of other configurations considered in the analyses. Contours reflect current density with darker shades reflecting lower current density. In particular the α′ particles are revealed due to the higher resistivity of the α′ phase.

Figure 7. These figures show difference between simulation and series resistor approximation: (a) simulation with random and fixed orientation, (b) size of α′ particles adjusted to 1/3, 2/3, and full size, and (c) simulation with eleven α′ particles in the model grain as shown in Figure 5(b).

Figure 8. This figure shows the combined results of simulations with different simulated α′ particle structures within the δ grains. These pooled simulations include those described in

Table 1. The various simulations are all with random orientation of the grains but included random limits on the amount of transformation, random numbers of δ grains that partially transformed within the 100 grain simulation, and simulations that include well-developed α′ particles within the δ grains. The aim is to compare possible microstructures that might evolve in different ways during the transformation. The observation from this plot is that the resistance obtained from the simulations does not significantly depend on an assumed path for the evolution of the α′ lenticular microstructure. Open circles represent the model shown by equation 1.

Figure 9. A simple flat plate α′ (dark plates) microstructure is shown in δ phase (light) with plates oriented vertically and horizontally with an equal proportion oriented vertically and horizontally. This is effectively the equivalent to the average of the series and parallel approximation. (The bars at top and bottom provide two equipotential surfaces for the illustration.)

Figure 10. This figure provides a comparison of parallel plate simulation with the series, parallel, and the average of series and parallel approximation. The squares are the series approximation, the triangles are the parallel approximation, and the large open circles are the average of the series and parallel approximation. Closed circles are the result of a simulation with varying amount of α′ in the parallel plate microstructure shown in Figure 9.

Figure 11. This figure shows the pooled simulation results (small diamonds) from Figure 8 (obtained from simulated microstructures in Figures 5 and 6) overlaid upon the results from the simulation of parallel plate microstructure (small circles) from Figure 10 (obtained from the

simulated microstructure in Figure 9). The line marking the average of the series and parallel approximations as well as the data from Figure 10 (parallel plate simulation) is mostly obscured by the data from the pooled simulation results.

FIGURES

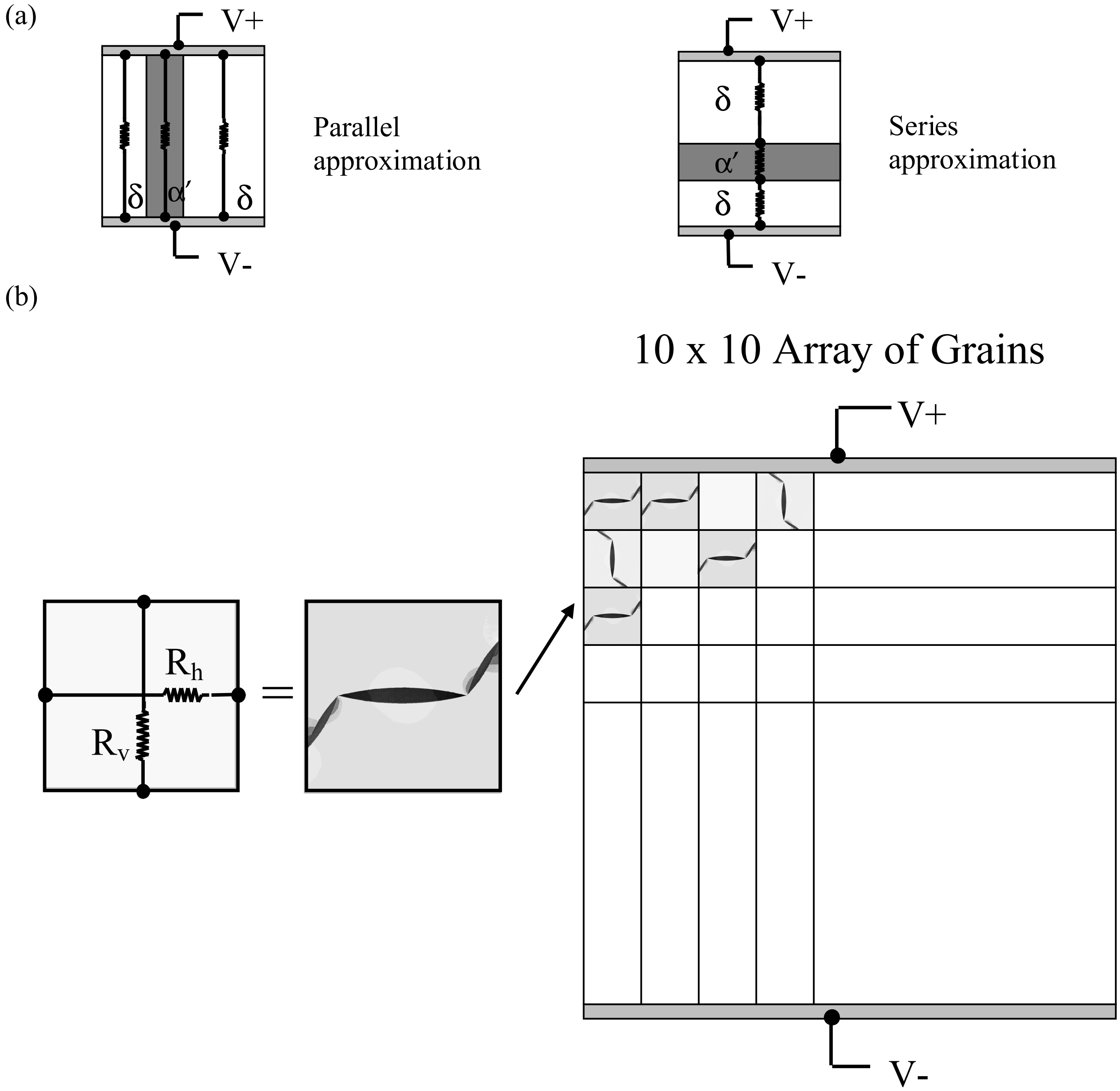

Figure 1. (a) These illustrations show the conceptual microstructure and resistor network for the series and parallel approximation. The resistor equivalent circuit is shown superimposed on the simulated microstructure. The thin bars on the top and bottom provide two equipotential surfaces. (b) These figures show the equivalent electrical circuit determined from a finite element simulation of a lenticular α′ microstructure. The illustration on the right shows a simulation with a 10 x 10 array of simulated grains. A resistor network with resistance values R_v and R_h obtained for each grain was used for the simulations of the microstructure. Depending on the simulation, the grains would be assigned randomly as containing transformed α′ and also in some cases the amount of α′ in the grain.

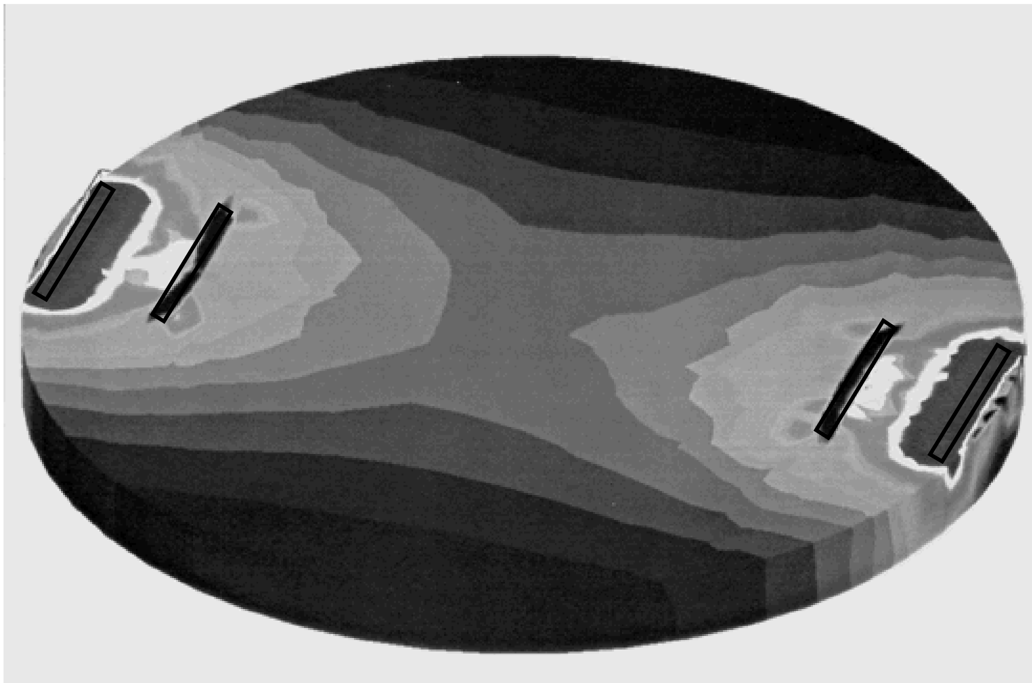

Figure 2. This figure shows a finite element simulation of the current flow through the disk. The rectangular boxes show the locations and length of the wires contacting the top of the sample for the 4-probe resistivity measurements. The highest current density is under the end (current) electrodes with intermediate current density in the middle of the disk. Less current density is found in the darker edges away from the electrodes.

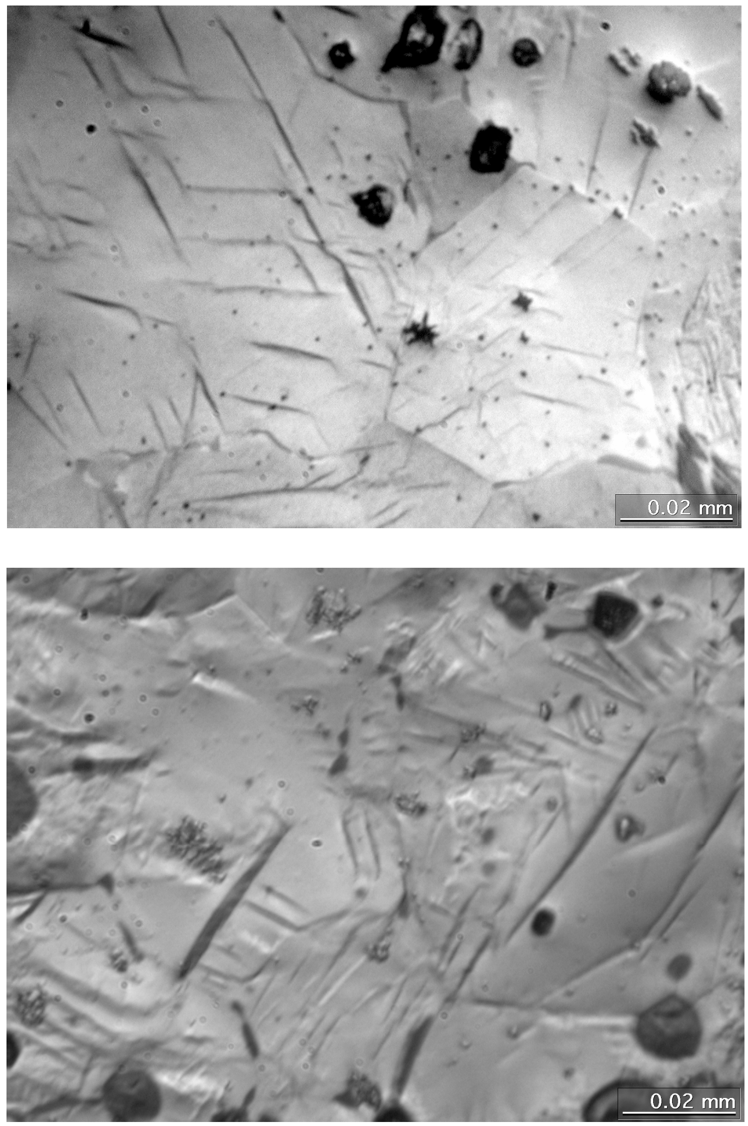

(a)

(b)

Figure 3. (a) Optical micrograph of partially transformed δ grains with α′ particles revealed with differential interference contrast. White and black elongated particles are α′. Sample was held at –118°C for 1000 seconds to produce the α′ particles. The volume fraction of α′ particles in the micrograph in Figure 3(a) is 6.9 volume % with an aspect ratio of approximately 9. The thickness dimension was 0.9 μm on average. (b) This figure shows a microstructure after cooling to -120°C at ~20°C/minute to transform δ to α′.

(a)

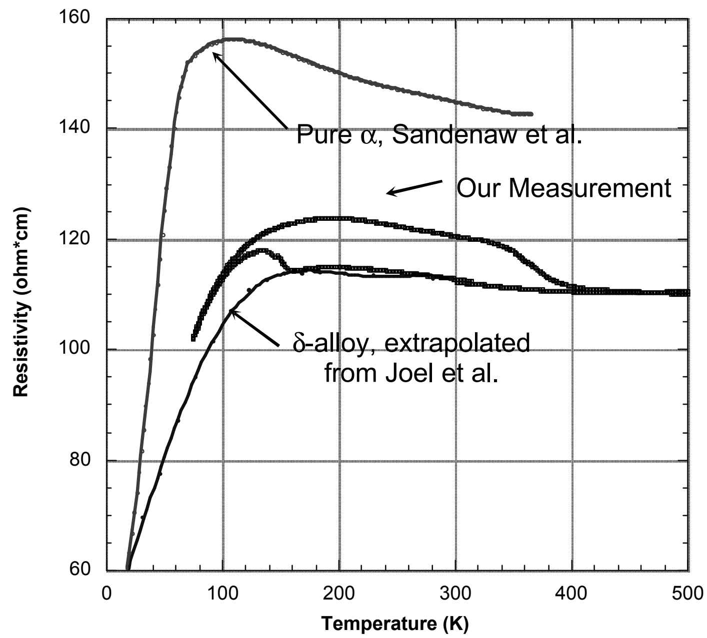

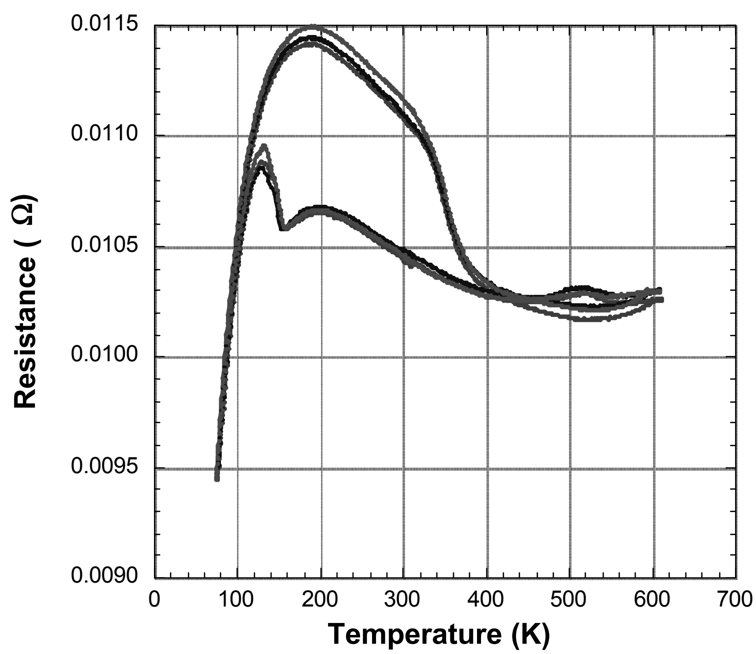

(b)

Figure 4. (a) Resistivity measured on a Pu-Ga alloy using 4-probe resistivity on a disk sample. The resistivity of α and δ phases is also shown for reference. (b) Measurement of resistance on several cycles at 1.5K/minute for the same sample.

(a) (b)

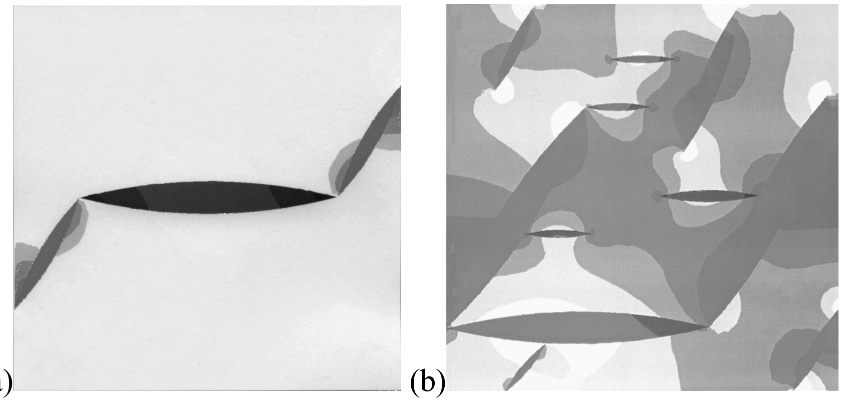

Figure 5. This illustration shows simulated microstructures of (a) Thin lens α', (b) 11 lens configuration of α'. Darker areas reflect a lower current density. Dark lens shapes are the α' which has a higher resistivity compared to the delta phase. The α' particles are the simple lens shaped objects in these illustrations.

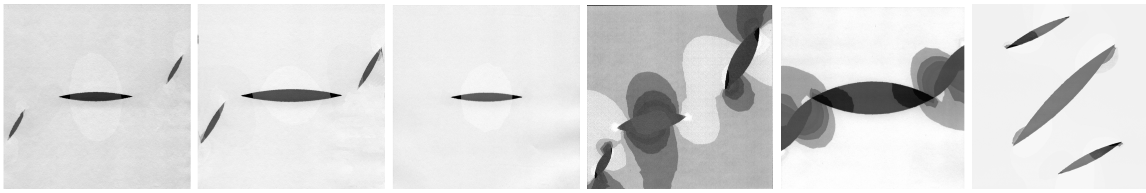

Figure 6. Additional α′ lens shape configurations used for further analyses. The first two were simulations of the configuration in Figure 5 (a) at earlier times in the α′ particle growth. The other four are examples of other configurations considered in the analyses. Contours reflect current density with darker shades reflecting lower current density. In particular the α′ particles are revealed due to the higher resistivity of the α′ phase.

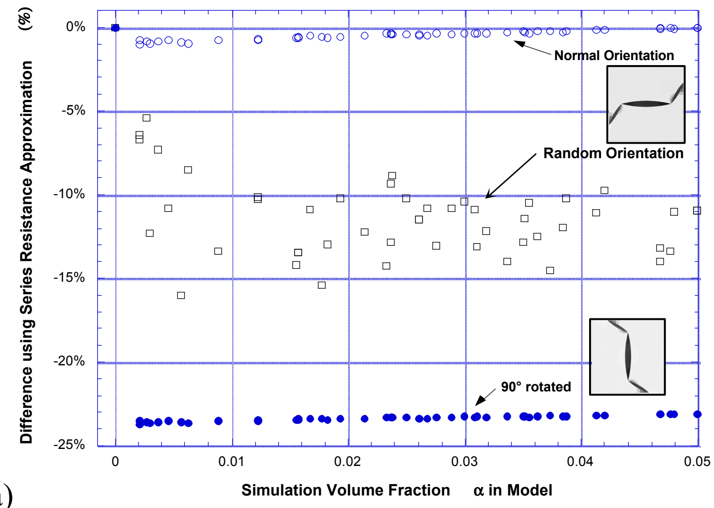
Difference using Series Resistance Approximation (%)
0%
-5%
-10%
-15%
-20%
-25%
Normal Orientation
Random Orientation
90° rotated
0
0.01
0.02
0.03
0.04
0.05
Simulation Volume Fraction α in Model

(a)

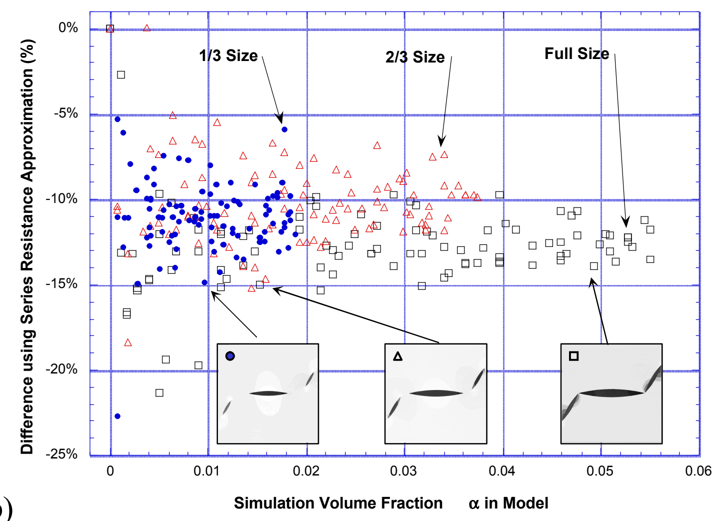
Difference using Series Resistance Approximation (%)
0%
-5%
-10%
-15%
-20%
-25%
1/3 Size
2/3 Size
Full Size
0
0.01
0.02
0.03
0.04
0.05
0.06
Simulation Volume Fraction α in Model

(b)

(c)

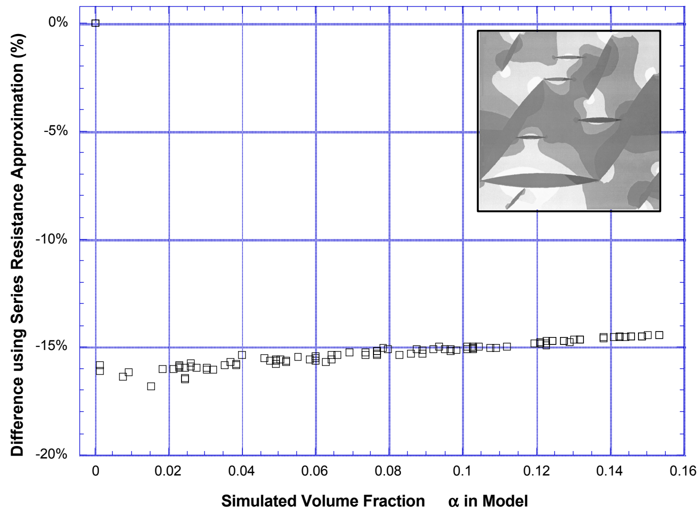

Figure 7. These figures show difference between simulation and series resistor approximation: (a) simulation with random and fixed orientation, (b) size of α′ particles adjusted to 1/3, 2/3, and full size, and (c) simulation with eleven α′ particles in the model grain as shown in Figure 5(b).

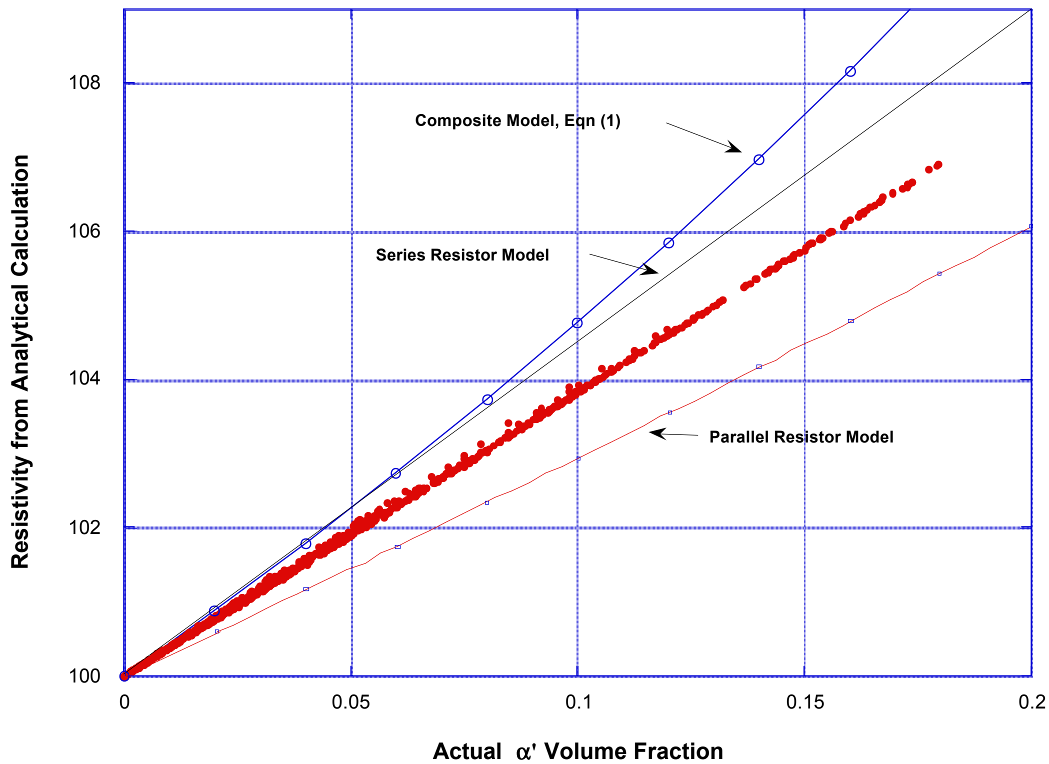

Figure 8. This figure shows the combined results of simulations with different simulated α' particle structures within the δ grains. These pooled simulations include those described in Table 1. The various simulations are all with random orientation of the grains but included random limits on the amount of transformation, random numbers of δ grains that partially transformed within the 100 grain simulation, and simulations that included well-developed α' particles within the δ grains. The aim is to compare possible microstructures that might evolve in different ways during the transformation. The observation from this plot is that the resistance obtained from the simulations does not significantly depend on an assumed path for the evolution of the α' lenticular microstructure. Open circles represent the model shown by equation 1.

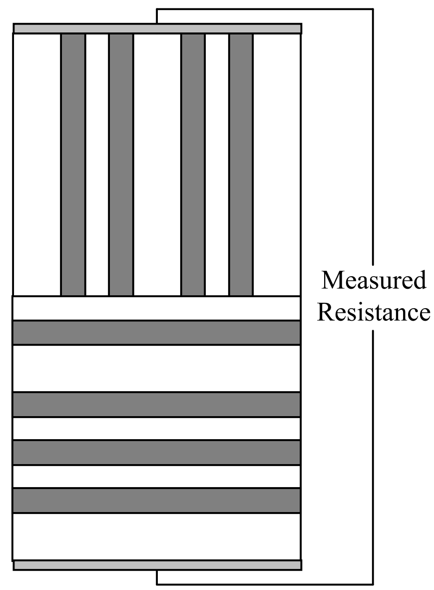

Figure 9. A simple flat plate α′ (dark plates) microstructure is shown in δ phase (light) with plates oriented vertically and horizontally with an equal proportion oriented vertically and horizontally. This is effectively the equivalent to the average of the series and parallel approximation. (The bars at top and bottom provide two equipotential surfaces for the illustration.)

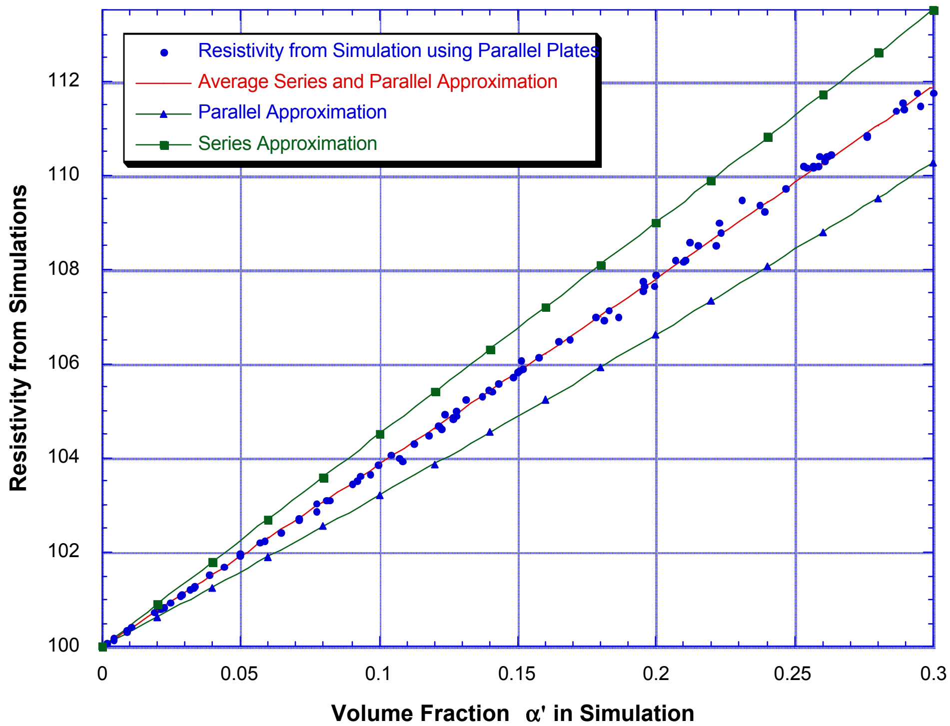

Figure 10. This figure provides a comparison of parallel plate simulation with the series, parallel, and the average of series and parallel approximation. The squares are the series approximation, the triangles are the parallel approximation, and the large open circles are the average of the series and parallel approximation. Closed circles are the result of a simulation with varying amount of α′ in the parallel plate microstructure shown in Figure 9.

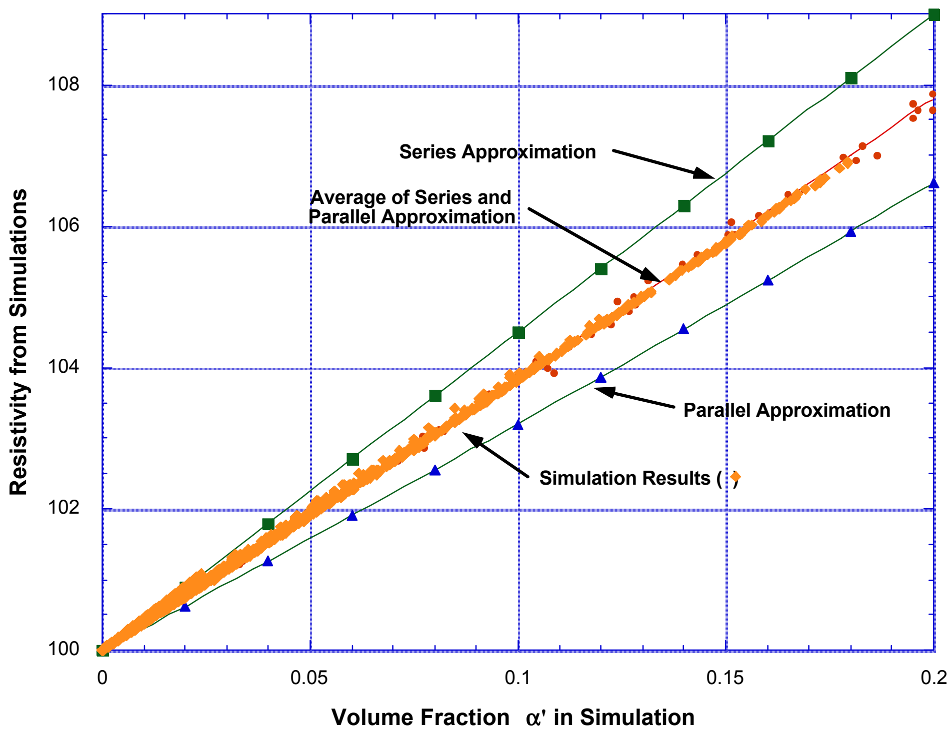

Figure 11. This figure shows the pooled simulation results (small diamonds) from Figure 8 (obtained from simulated microstructures in Figures 5 and 6) overlaid upon the results from the simulation of parallel plate microstructure (small circles) from Figure 10 (obtained from the simulated microstructure in Figure 9). The line marking the average of the series and parallel approximations as well as the data from Figure 10 (parallel plate simulation) is mostly obscured by the data from the pooled simulation results.